J-6-01 (Invited)

Extended Abstracts of the 2018 International Conference on Solid State Devices and Materials, Tokyo, 2018, pp585-586

Applications of chemical imaging sensor in the field of electrochemistry

Ko-ichiro Miyamoto[1] and Tatsuo Yoshinobu[1,2]

[1] Department of Electronic Engineering and [2] Department of Biomedical Engineering
Tohoku University, 6-6-05 Aramaki Aza Aoba, Aoba-ku
Sendai city, 980-8579, Japan
Phone: +81-22-795-7075 E-mail: k-miya@ecei.tohoku.ac.jp

Abstract

Chemical imaging sensor is a semiconductor device based on the field effect to visualize the ion distribution in a sample solution. In addition to its applications to biological samples and microfluidics, we recently proposed novel applications of the chemical imaging sensor in the field of electrochemistry. With the flat sensor surface placed in the vicinity of a stainless steel surface, initiation and propagation of crevice corrosion were successfully visualized *in situ*. It was also demonstrated that the sensor was capable of visualizing hydrogen permeation in steel.

1. Chemical imaging sensor

The ion concentration is one of the most essential parameters in electrochemical and biochemical processes. However, label-free methods to observe the spatiotemporal changes of the ion distributions are very limited. A chemical imaging sensor (CIS) is a semiconductor device which is capable of visualizing the ion distribution in a sample solution [1]. Fig. 1 is a schematic view of the CIS measurement system consisting of a sensor plate, a scanning optics and an external circuit to record the photocurrent signal.

The CIS sensor is made of an n-type silicon plate (1 – 10 Ω·cm, t = 200 μm). First, 50 nm of thermal oxide is grown as an insulating layer, then the second insulating layer, 50 nm of silicon nitride, which functions also as a pH sensitive layer, is deposited by a CVD process. After that, the backside of the sensor plate is polished and gold electrodes are deposited to form ohmic contacts.

In a CIS measurement, the sensor surface is in contact with the sample solution, forming an electrolyte – insulator – semiconductor (EIS) structure. A DC bias voltage is applied between the sensor plate and a reference electrode dipped in

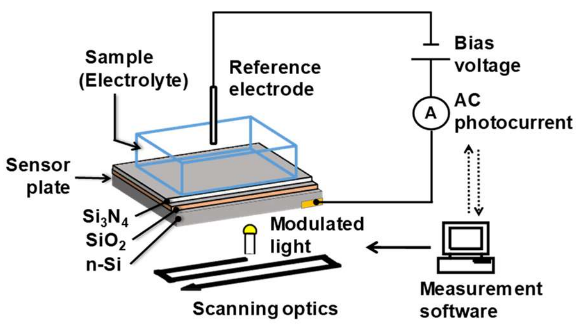

Fig. 1 Schematic view of the measurement system of chemical imaging sensor and the structure of the sensor plate.

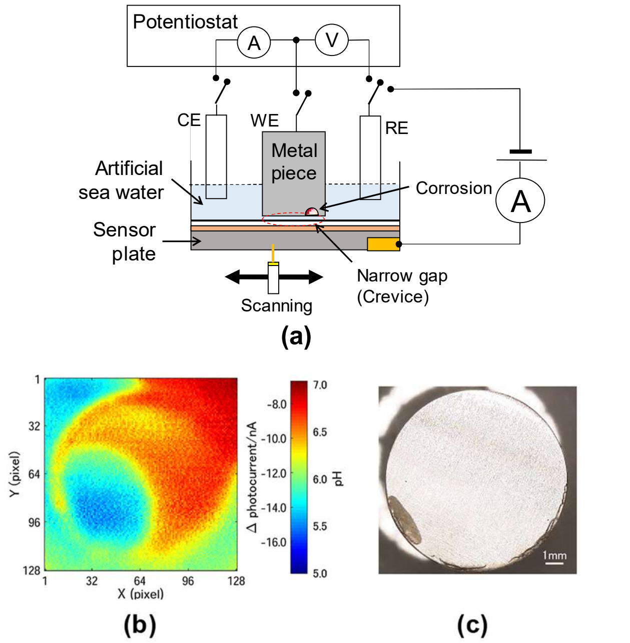

Fig. 2 (a) The measurement setup to observe the crevice corrosion of stainless steel. (b) Typical pH image inside the crevice. (c) Optical image of the corroded surface of the test piece after the experiment. ((b) and (c) were reproduced from [8].)

the sample solution to induce a depletion layer at the insulator – semiconductor interface.

Corresponding to the ion distribution in the sample solution, or pH distribution in case of protons, the charge on the sensor surface becomes spatially distributed, which in turn exerts a field effect and modulates the thickness of the depletion layer. To read out the spatial distribution of the capacitance of the depletion layer, a focused and modulated light beam scans the backside of the sensor plate, which generates an AC photocurrent signal depending on the local capacitance and therefore on the ion concentration at the location illuminated.

The CIS has many advantages such as being label-free and flexible in the choice of scan patterns. In addition, the sensor surface is flat and uniform without any structures. Based on these advantages, various applications have been proposed. In the field of biology, for example, metabolic activities of bacteria [2] and neuronal cells [3] were measured. Recently, a defect of a cell layer in its recovery process was visualized [4]. By fabricating a microfluidic channel on the sensor surface, the product of an enzymatic reaction [5] and ion diffusion across the boundary of laminar flows [6] were

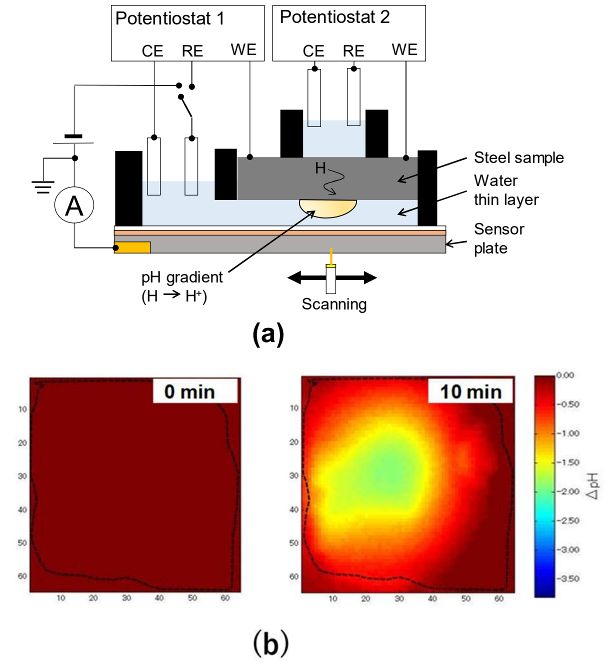

Fig. 3 (a) The measurement system to detect the hydrogen permeation in steel. (b) pH change due to protonation of H atoms.

visualized. This paper focuses on the application of CIS to visualization of electrochemical reactions on metal surfaces.

2. Applications of chemical imaging sensor

In-situ visualization of crevice corrosion

Stainless steel is a common material widely used in industry with a strong corrosion resistance due to the native passivation layer of chromium oxide. However, under certain conditions such as in a narrow gap in water environment, the passivation layer is damaged by lowering of pH caused by hydrolysis of chromium, which triggers corrosion. This phenomenon is known as 'crevice corrosion'. Although the importance of crevice corrosion has long been recognized, *in-situ* observation inside a narrow crevice (typically on the scale of microns) has been difficult.

We applied CIS to the monitoring of crevice corrosion [7, 8]. The concept of the measurement is shown in Fig.2a. A very flat sensor surface of CIS is ideal to face the polished surface of metal under test forming a narrow gap. The potential of the test piece was controlled by a potentiostat to accelerate the corrosion. Fig. 2b shows an example of pH distribution after corrosion of the test piece, which was a cylindrical stainless steel (SUS304, 12 mm in diameter). A local decrease of the pH value was observed at the lower left corner of the image, which corresponded to the corrosion site observed in the optical image in Fig. 2c.

The measurement system was further developed to minimize the interference between the anodic current of corrosion and the AC photocurrent signal of CIS measurement, which enabled time-lapse imaging of spatiotemporal change of pH distribution in the course of propagation of corrosion in a crevice [8].

Label-free visualization of hydrogen permeation in steel

Recently, 'high tensile strength steel (HTSS)' is extensively used in car industry. In spite of its enhanced strength, the risk of hydrogen embrittlement in HTSS is also known. Permeation of hydrogen atoms into steel, which is sometimes initiated by corrosion, and subsequent diffusion of hydrogen atoms eventually cause crack or fracture of the steel. However, the methods of evaluation and visualization of hydrogen permeation in steel have been limited.

Fig. 3a depicts the novel measurement setup of CIS to visualize hydrogen permeation. A steel sample is placed above the sensor surface with a gap filled with water. The steel sample was charged with hydrogen from the top side by cathodic polarization using the potentiostat 2. After charging, the bottom surface of the steel sample was anodically polarized by the potentiostat 1 to protonate the hydrogen atoms that reached the bottom surface by diffusion through the sample. Fig. 3b shows the pH changes during the anodic polarization of the steel sample. A local decrease of the pH value was observed at around the center of the scanning area, which corresponded to the area of hydrogen charging. The amount of protons estimated from the pH image was comparable with the net charge calculated by integration of anodic current.

3. Conclusions

A CIS can be applied to various types of measurements; not only those of biological samples but also those of electrochemical phenomena. A CIS has been successfully applied to *in-situ* observation of crevice corrosion of stainless steel, in which the lowering of pH at the corroded site was visualized. A CIS was also applied to visualization of hydrogen permeation in steel. The distribution of protons generated by ionization of hydrogen atoms that diffused through a steel sample was successfully visualized.

Acknowledgements

A part of this study was supported by JSPS KAKENHI Grant Number 17H03074 and JFE 21st Century Foundation.

References

[1] M. Nakao, T. Yoshinobu and H. Iwasaki, Sens. Act. B **20** (1994) 119.
[2] H. Iwasaki and T. Yoshinobu, OYOBUTURI **66** (1997) 488.
[3] H. Tanaka, T. Yoshinobu and H. Iwasaki, Sens. Act. B **59** (1999) 21.
[4] K. Miyamoto, B. Yu, H. Isoda, T. Wagner, M.J. Schöning and T. Yoshinobu, Sens. Act. B (2016) 965.
[5] K. Miyamoto, Y. Hirayama, T. Wagner, M.J. Schöning and T. Yoshinobu, Electrochim. Acta **113** (2013) 768.
[6] K. Miyamoto, H. Ichimura, T. Wagner, M.J. Schöning and T. Yoshinobu, Sens. Act. B **189** (2013) 240.
[7] K. Miyamoto, S. Sakakita, T. Wagner, M.J. Schöning and T. Yoshinobu, Electrochim. Acta **183** (2015) 137.
[8] K. Miyamoto, S. Sakakita, C.F. Werner and T. Yoshinobu, phys. status solidi A (2018) 1700963.